IEEE Access
Multidisciplinary | Rapid Review | Open Access Journal

Received July 26, 2021, accepted August 27, 2021, date of publication September 6, 2021, date of current version September 17, 2021.

Digital Object Identifier 10.1109/ACCESS.2021.3110715

On-Body UWB Channel Classification and Characterization for Various Physical Exercises

RICHA BHARADWAJ, (Member, IEEE), AND SHIBAN K. KOUL, (Life Fellow, IEEE)
Centre for Applied Research in Electronics, Microwave and RF Group, Indian Institute of Technology Delhi, New Delhi 110016, India

Corresponding author: Richa Bharadwaj (richab@iitd.ac.in)

This work involved human subjects or animals in its research. The authors confirm that all human/animal subject research procedures and protocols are exempt from review board approval.

ABSTRACT This paper presents classification, characterization and modelling of ultra-wideband (UWB) on-body channel links while performing various physical exercises. The physical exercises mainly focus on range-of-motion exercises in which the upper and lower limb movement is dominant. Such exercises are suitable for various applications in medical domain such as rehabilitation, physiotherapy, in sports for training and general-well-being. Wrist and ankle regions have been chosen for the wearable antenna placement and three different antenna orientations have been considered with respect to the location on the limb, inner, outer, and front region. The channel for various activities has been classified into line of sight (LOS) and non-line of sight (NLOS) links based on computation of Kurtosis. On-body statistical analysis and distance-dependent study is performed on two important channel parameters, path loss magnitude and rms delay spread considering the LOS and NLOS links. The channel variation is attributed to the location/orientation of the antenna, Tx-Rx distance, obstruction caused by the human body and different categories of activities.

INDEX TERMS Ultra-wideband, channel classification and characterization, compact antenna, physical activities.

I. INTRODUCTION

Physical activities and exercises are part of day-to-day life and application specific domains such as physiotherapy, rehabilitation, and sports training. Monitoring and classification of physical activities through various types of sensors has gained a lot of interest due to the miniaturization of wearable devices and advancement in wireless communication technologies [1]. Several types of technologies such as Optical, Inertial and RF based technologies are reported in open literature and in commercial domain for monitoring and tracking physical activities, postures, and movements [2], [3]. Camera-based optical technologies are gold standard for motion monitoring but are very expensive, have privacy issues, suffer from occlusion, and preferred in lab-based environment [4], [5]. Inertial sensors are relatively cheap and commercially available but suffer from calibration and drift errors [4], [5].

Among RF technologies, Ultra-Wideband (UWB) technology is very suitable for wearable communication applications such as human localization, tracking and activity monitoring [6]–[10]. UWB has attractive features such as fine time resolution, low cost, low power, robustness to multipath, compact antenna design and integration with other technologies [11]–[14]. An important aspect of the UWB body-centric communication is channel characterization of the wearable nodes which vary with different locations on the body, postures, and physical activities [15], [16]. Hence, it is necessary to obtain accurate classification, characterization, and statistical analysis of the body-centric links to optimize wireless devices and antennas for UWB WBAN applications [17], [18].

UWB on-body channel analysis has been performed for static scenarios with focus on the torso region in [19]–[23] and various body locations in [24]. The on-body channel measurements and modelling using compact wearable antennas has been carried out in [19]–[23]. Generally, the Tx antenna is placed on the torso region and the Rx nodes are located over different regions of the human subject such as front/back torso region, head and limb locations like wrist, shoulder, thigh etc. [19]–[24]. Pseudo dynamic mode and posture related on-body channel characterization has been carried out

The associate editor coordinating the review of this manuscript and approving it for publication was Chinmoy Saha.

in [25]–[27]. In [25] four different on-body channels were investigated with the human subject performing swinging and random movements in the 3-9 GHz frequency range. The Tx was placed on the belt and Rx locations considered were head, chest, wrist, and ankle. Walking activity is performed by a human subject in an indoor environment with the UWB wearable antennas placed on different locations in [26]. Path loss (PL) is analyzed for the different positions for 3-5 GHz frequency range during the walking activity. Work reported in [27] presents PL analysis in the 3.1-10.6 GHz for the arm and leg swinging movement with the receiver antenna mounted on the waist and Tx antenna mounted on the wrist/ankles.

This paper presents experimental investigations regarding on-body channel classification and characterization while performing different physical exercises with the focus on the upper limbs and lower limbs channel. As the human subject performs different limb movements, the human channel varies significantly [5]. Hence, different types of links are formed such as line-of-sight (LOS) and non-line-of-sight (NLOS) links, which have been accurately classified through Kurtosis. Apart from channel classification for various limb movements, statistical analysis is carried out for two commonly used channel parameters namely PL and rms delay spread (σ_τ). Channel models have also been derived for PL and σ_τ corresponding to different orientations of the wearable antenna and LOS/NLOS links.

To the best of authors knowledge on-body channel classification, characterization, and modelling of the upper and lower limb movements during various physical exercises is very limited. The channel information and statistical analysis reported can aid in smart methodologies and algorithms for wearable activity monitoring devices. The rest of this paper is organized as follows. The measurement set-up in an indoor environment for on-body measurements is presented in section II. The channel classification for upper and lower limb movements is presented in section III. Channel characterization and statistical analysis is presented in section IV and channel modeling with respect to distance is presented in section V. The key findings are reported in context with the channel variation in the same section. Finally, the conclusion is presented in section VI with highlights on the future aspects.

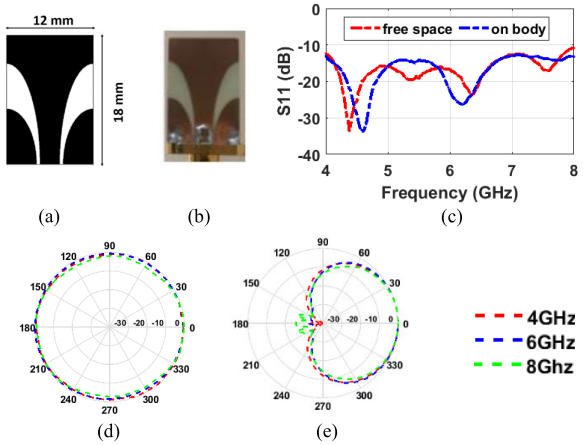

FIGURE 1. Mini-TSA antenna (a) schematic (b) fabricated structure. (c) S_{11} for free space and on-body scenarios. Azimuth radiation pattern for (d) free space and (e) on-body scenario.

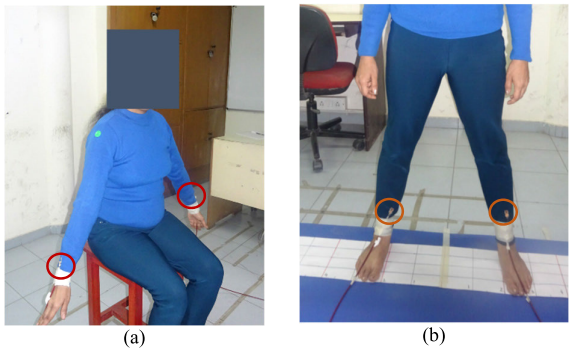

FIGURE 2. Human subject performing (a) upper limbs and (b) lower limb activities with the wearable antennas placed on the wrist and ankle region.

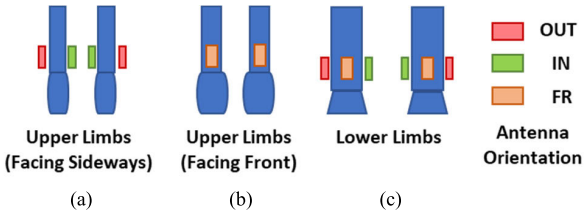

FIGURE 3. Various on-body antenna orientations (OUT, IN, FR) during upper limb activities (a) Arm facing sideways, (b) Arm facing front and lower limb activities (c) Legs facing front.

II. MEASUREMENT SET UP

Measurements are performed on real human subject in an indoor environment in the 4-8 GHz frequency range and using compact mini-tapered slot antennas (TSA) 12 × 18 mm^2 [5] inspired from [19] which are placed on specific locations on the limbs. The mini-TSA (Fig. 1 (a) and (b) schematic and fabricated structure) has good performance in free space and on-body in the desired frequency band (Fig. 1 (c)-(e)). A female human subject with height of 160 cm and average built is considered for performing upper and lower limb movement activities. Fig. 2 (a) and (b) show the wearable antenna placed on the left/right (L./R.) wrist (WR) and ankle (AK) respectively. Three orientations of the antenna are considered namely, facing outward (OUT), inward (IN) and front (FR) as depicted in the schematic shown in Fig. 3. Several exercises related to both limb movements, single limb movements and limb bending are carried out with the schematics presented in Fig. 4 (a) and (b) with details given in [5].

Range of motion activities [28], [29] are performed in different *x-y*/*y-z*/*x-z* planes and several angles (at interval of 30°/15°) which lead to different displacement distance. Summary of the wearable antenna location and that of the reference is presented in Table 1. For both, single upper/lower

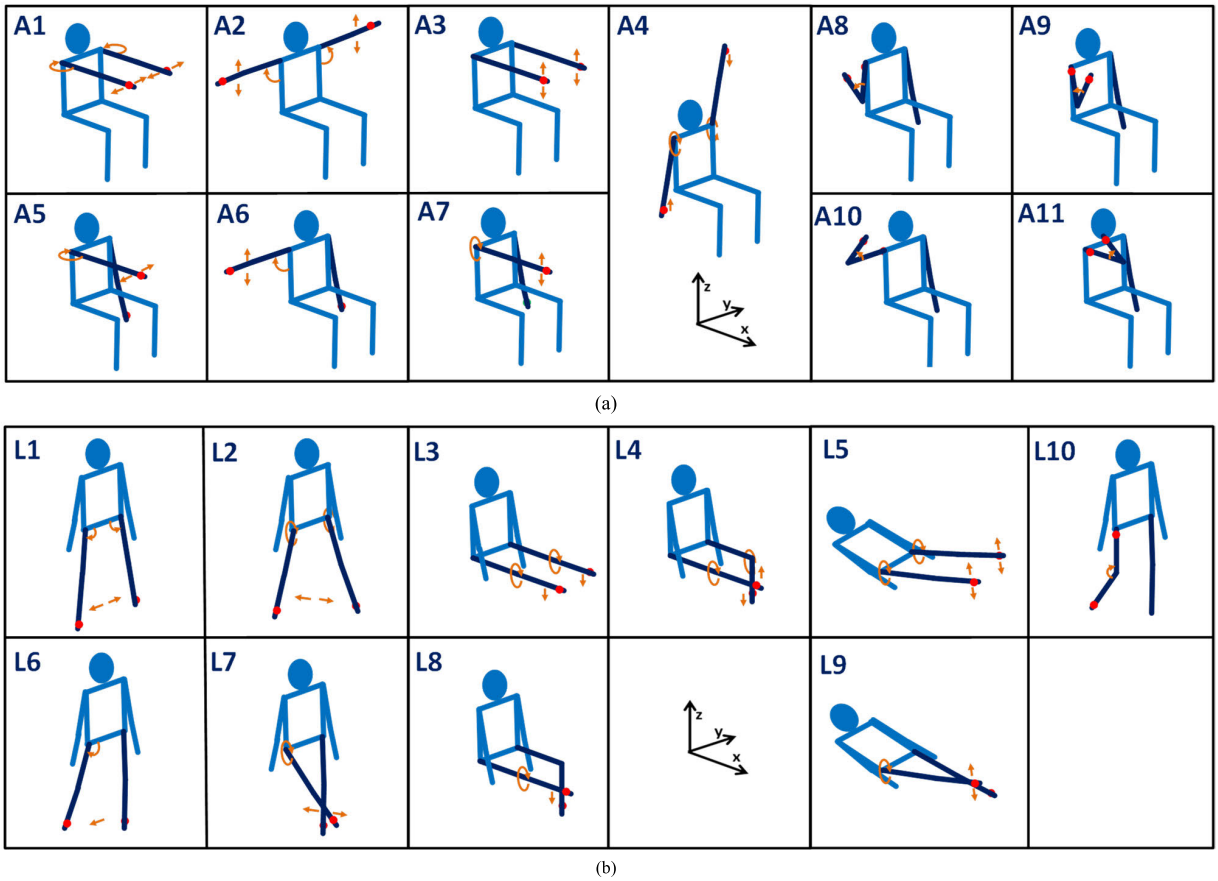

FIGURE 4. (a) Upper limb movement activity: Both arms movement (A1-A4), Single arm movement (A5-A7), arm bending (A8-A11), (b) Lower limb movement activity: Both legs movement (L1-L5), Single leg movement (L6-L9), Leg bending (L10).

TABLE 1. Limb exercise details and categories.

	Antenna Location	Plane	Reference
Upper Limbs Activity			
Both Arms (A1-A4)	L. WR-R. WR	*x-y/x-z/y-z*	Shoulder
Single Arm (A5-A7)	L. WR-R. WR	*x-y/x-z/y-z*	Shoulder
Arm Bend (A8-A11)	R. SH-R. WR	*x-z/y-z*	Elbow
Lower Limbs Activity			
Both Legs (L1-L5)	L. AK-R. WR	*x-z/y-z*	Thigh
Single Leg (L6-L10)	L. AK-R. WR	*x-z/y-z*	Thigh
Leg Bend (L11)	R. TH-R. WR	*x-z*	Knee

limb movements the reference angle is with respect to the shoulder/thigh (SH/TH) region and for bending movement, the elbow/knee (EL/KN) joint is the reference.

The wearable antennas are connected to the two-port vector network analyser (VNA) using low loss flexible cables to provide freedom in limb movement activities. The sweep is performed over 1601 frequency points in the 4-8 GHz range. Data is recorded at different positions for each activity for which the 30°/15° displacement and the positions are estimated through digital protractor with respect to the reference joint. The measured magnitude and phase of the S_{21} is converted to the time domain by applying an inverse fast Fourier transform (IFFT) to determine the channel impulse response (CIR). Further convolution is carried out with the UWB Gaussian pulse to obtain the received pulse.

III. CLASSIFICATION OF THE ON-BODY CHANNELS

Channel classification assists in obtaining important information related to the propagation phenomenon occurring between two wearable links. It provides information regarding good (LOS) and bad (NLOS) links related to the wearable antenna location. The variable nature of the body during physical exercises forms different types of on-body channel characteristics leading to obstructed and non-obstructed links. Kurtosis is one such channel parameter which aids in evaluation of the channel in terms of LOS/NLOS, gives an idea of certain channel properties, hence, provides guidelines for the design and development of channel/time of arrival (TOA) estimation algorithms [14], [30]. Kurtosis κ is mathematically defined as follows:

$$\kappa(x) = \frac{1}{\sigma^4} \frac{\sum_i (x_i - \bar{x})^4}{N} \tag{1}$$

where σ is the standard deviation of the variable x and $\bar{x}$ is the mean value of x. N is the number of samples of x.

A channel impulse response (CIR) with high κ, classifies as LOS links and for NLOS links, κ will be lower due to high multipath and low magnitude. The wearable antennas are

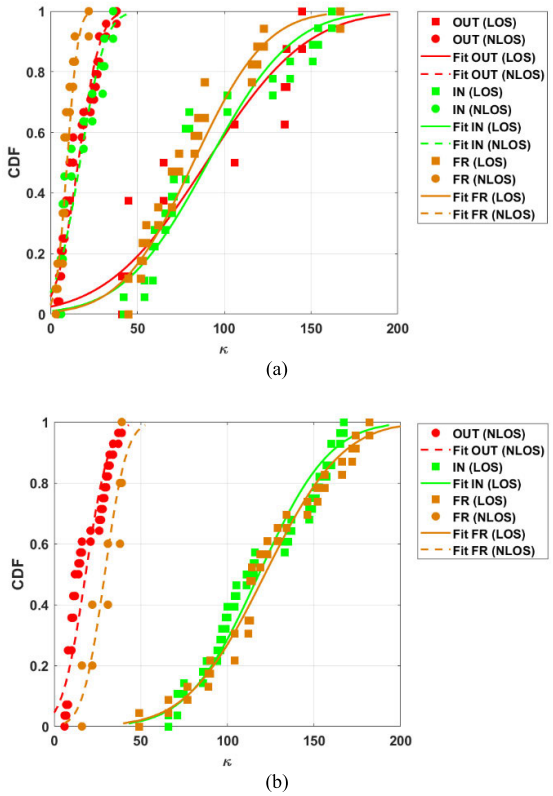

FIGURE 5. CDFs for Kurtosis based channel classification (LOS and NLOS) considering antenna orientation: OUT, IN, WR. Both limbs movement: (a) Upper limbs (b) Lower limbs. Solid line represents LOS links and dotted line represents NLOS links.

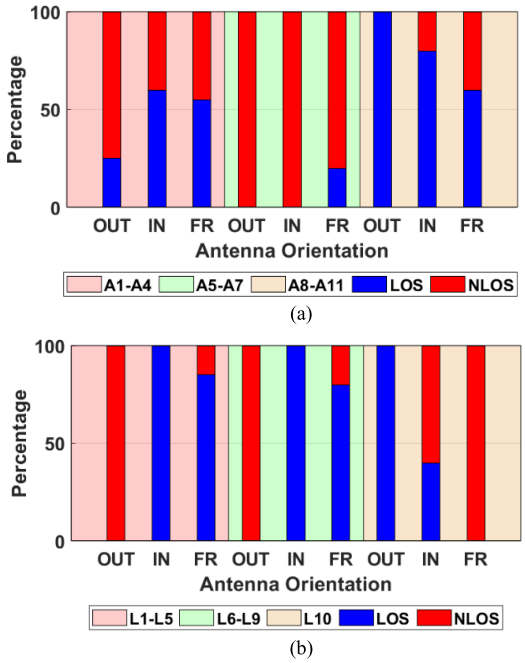

FIGURE 6. Stacked bar graph representing percentage of LOS and NLOS on-body links classified during various (a) upper and (b) lower limb activities for antenna orientations corresponding to OUT, IN, FR and different activity categories.

placed on the left (L.) wrist/ankle and right (R.) wrist/ankle for the activities considered as shown in Fig. 4(a) and (b) respectively. Figure 5(a) and (b) presents Cumulative Distribution Function (CDF)s of the obtained classification results for both arms (A1-A4) and legs movement (L1-L5) activities. Different antenna orientations OUT, IN, WR are considered and LOS/NLOS links are reported based on the measurement data. Generally, κ in the range of 50-200 are in LOS situation due to high peakedness of the CIR. For NLOS/partial NLOS links, κ is very low ranging from 5-20 for total NLOS and 20-40 for partial NLOS links. The percentage of classification of LOS and NLOS links is presented in Fig. 6 (a) and (b) for all the categories of the upper and lower limb activities respectively based on Kurtosis considering different wearable antenna orientations OUT, IN and FR.

A. UPPER LIMBS ACTIVITY

The wearable antennas are placed on the left (L.) wrist and right (R.) wrist for both arm movement (A1-A4) activities as shown in Fig. 4 (a). For OUT_WR antenna orientation, 25 % LOS links are observed and 75 % NLOS links are observed. The IN_WR orientation has maximum number of LOS scenarios while performing upper limb activities, due to the higher occurrence of direct LOS path. For the FR_WR orientation, there are more LOS links than NLOS by 5 %. which can be seen in the % classification results presented in Fig. 6 (a).

For single arm movement (A5-A7), right arm is performing the activity and the left arm is at rest which can be seen in the schematics presented in Fig. 4 (a). Total NLOS situations are observed for single arm movement for OUT_WR and IN_WR antenna orientation due to obstruction caused by the torso/thigh region. For the case of FR_WR orientation of the wrist, there are 20 % chances of LOS scenarios for the activities performed and rest 80 % links formed are NLOS/partial NLOS scenarios. During arm bending activities A8-A11, one of the antennas is placed on the outer region of the shoulder, the other antenna is placed on the wrist in three different orientations. OUT_WR has occurrence of total LOS links. For IN and FR orientation, 60-80 % LOS and 20-40 % NLOS links are observed.

B. LOWER LIMBS ACTIVITY

For both leg movements, the wearable antennas are placed on the ankle region for different antenna locations as shown in Fig. 4 (b). Considering L1-L5 activities, the OUT_AK orientation has total NLOS links due to obstruction caused from the legs, for IN_AK total LOS links are observed due to the direct path propagation between the Tx and Rx, FR_AK orientation leads to a 85 % LOS links and 15 % partial NLOS links which occur due to the transition from LOS $\rightarrow$ NLOS while performing limb movement activity.

In single limb movement activities, the left leg is in static position with the wearable antenna placed on the ankle region and the right leg is performing various movements, L6-L10 as

presented in Fig. 4 (b). Similar classification is observed as that of both leg movement activities with OUT_AK having total NLOS links, IN_AK with total LOS links and FR_AK generally having LOS links and few NLOS links as shown in Fig. 6 (b). For the leg bending scenario, both the antennas are placed on the right leg as depicted in Fig. 4 (b). The OUT_AK has total LOS links, IN_AK has 40 % LOS links due to the respective orientations of the wearable antenna placed on the ankle. FR_AK has no LOS links due to the obstruction caused by the shank/thigh, which corresponds to the channel type dependency on the antenna placement.

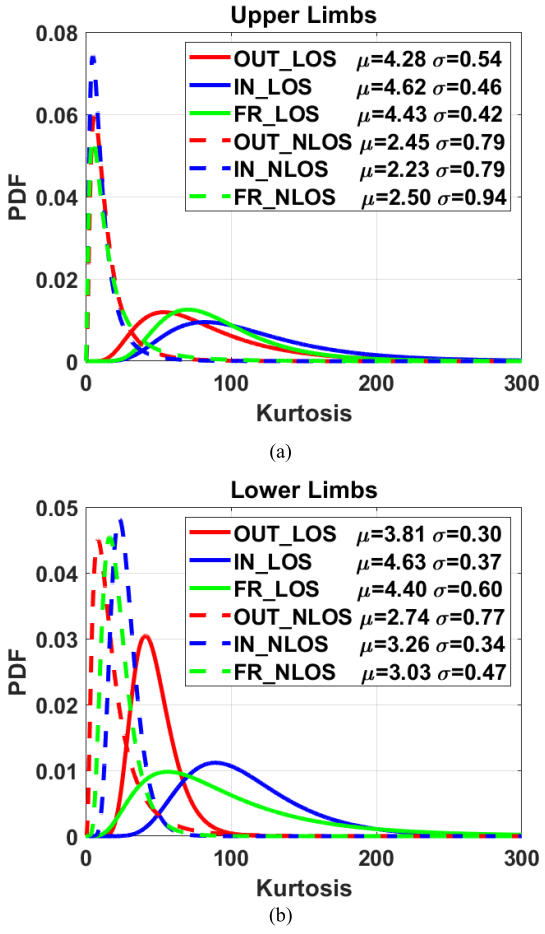

FIGURE 7. Log-normal PDFs of Kurtosis for various on-body antenna orientations (OUT, IN, FR) during (a) Upper limb activities and (b) Lower limb activities. Solid line represents LOS links and dotted line represents NLOS links.

C. KURTOSIS ANALYSIS BASED ON WEARABLE ANTENNA ORIENTATION

Fig. 7 represent log-normal probability density function (PDF)s of Kurtosis for various on-body antenna orientations for all the activity types for upper and lower limb activities. The log-normal PDF parameters μ and σ [18] are presented in each plot for the LOS and NLOS links which vary depending on various factors such as the channel type, orientation/location of the antenna. The PDF of the log normal distribution with parameters μ and σ is given as:

$$f(x) = \frac{1}{x\sigma\sqrt{2\pi}} e^{-\frac{(\ln(x)-\mu)^2}{2\sigma^2}} \tag{2}$$

As observed in Fig. 7 (a) the PDF spread is highest for IN_LOS links and lowest spread is observed for IN_NLOS links for upper limb activities. Considering lower limb movement activities analysis in Fig. 7 (b) for Kurtosis, maximum spread is observed for FR_LOS and minimum for IN_NLOS.

IV. PATH LOSS AND RMS DELAY SPREAD STATISTICAL ANALYSIS

A. ON-BODY CHANNEL PARAMETER STATISTICS WITH RESPECT TO ACTIVITY TYPE

Two channel parameters PL and σ_τ are statistically analysed for all the activities and orientations considered. The path loss is obtained as mean path gain over the measured frequency band, as shown in the equation [31]:

$$PL(d(p)) = -20.log_{10}\left\{\frac{1}{10}\frac{1}{N_f}\sum_{j=1}^{10}\sum_{n=1}^{N_f}\left|H_j^p(n)\right|\right\} \tag{3}$$

where $PL(d(p))$ is the path loss at the position of p, at which the distance between the Tx and Rx is a function of the position p, thus the distance is denoted by $d(p)$. N_f is the number of frequency samples of the VNA. $H_j^p(n)$ is the measured S_{21} for the position p, j^{th} snapshot, and n^{th} frequency sample. The rms delay spread is given by σ_τ which describes the time dispersive properties of the channel (h) and [32] is defined as:

$$\sigma_\tau = \sqrt{\frac{\sum_k (\tau_k - \tau_m)^2 . |h(\tau_k; d)|^2}{\sum_k |h(\tau_k; d)|^2}} \tag{4}$$

where τ_k are the multipath delays relative to the first arriving multipath component and d is the separating distance between the Tx and Rx. The σ_τ is higher for NLOS links in comparison to LOS links due to high MPCs and spread of the channel for NLOS scenarios. For on-body communication the human subject is the main source of obstruction, which leads to spread of the signal and multipath components for the NLOS scenarios.

The mean and standard deviation (STDEV) values of PL and σ_τ have been presented in Fig. 8 (a) and (b) respectively for different activity categories and orientations of the on-body antenna. Fig. 9 (a) and (b) depict the mean and standard deviation values for the leg movement activities. Overall, the magnitude of PL and σ_τ is higher for the NLOS links in comparison to LOS links due to the significant attenuation caused by the obstructed path and presence of high multipath for NLOS scenarios. From the analysis it can be observed that the magnitude of PL and σ_τ for the lower limb activities has less magnitude in comparison to upper limb activities. This is because the on-body antennas on the upper limbs are often obstructed by the torso region during physical activities

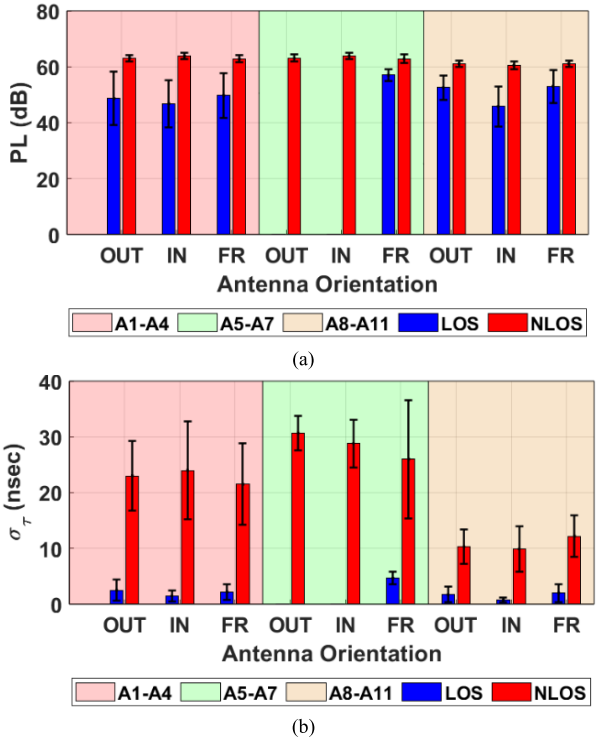

FIGURE 8. (a) Path loss magnitude and (b) RMS delay spread statistics (mean and STDEV) for LOS and NLOS links during upper limbs activities. Shaded region refers to the activity categories: Both arms movement (A1-A4), single arm movement: (A5-A7), bending arm movement: (A8-A11).

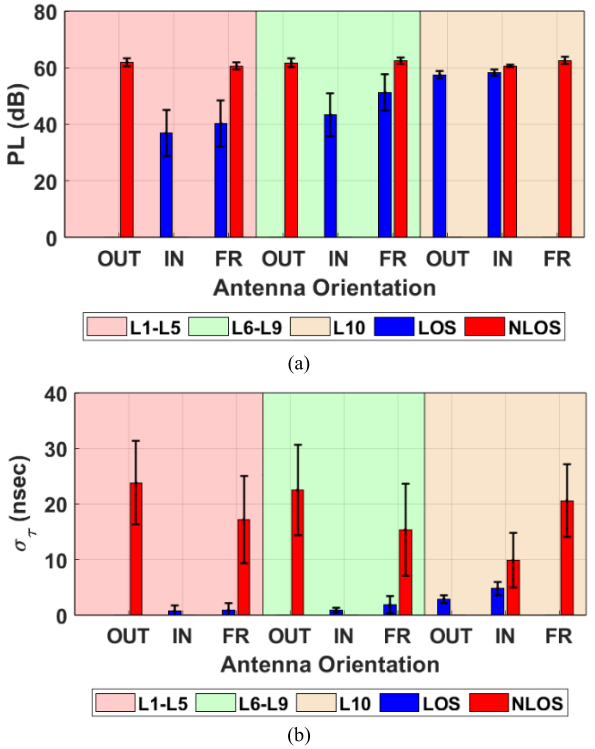

FIGURE 9. (a) Path loss magnitude and (b) RMS delay spread statistics (mean and STDEV) for LOS and NLOS links during lower limbs activities. Shaded region refers to the activity categories: Both legs movement (L1-A5), single leg movement: (L6-L9), bending leg movement: (L10).

which leads to NLOS links between the Tx-Rx. The distance between the Tx-Rx links also plays an important role in the magnitude of the channel parameters observed. During the physical activities performed, the displacement of the arms is higher for several activities in comparison to the lower limb activities leading to higher magnitude of PL and σ_τ. As observed from Fig. 8 (a) and Fig. 9 (a), the standard deviation is much larger for LOS links in comparison to NLOS links due to wider range of PL values obtained for LOS links. Considering the standard deviation values for σ_τ, higher variation is observed for NLOS links in comparison to LOS links as observed in Fig. 8 (b) and 9 (b).

B. ON-BODY CHANNEL PARAMETER STATISTICS WITH RESPECT TO WEARABLE ANTENNA ORIENTATION

Fig. 10 and Fig. 11 represent log-normal PDFs of PL and σ_τ for various antenna orientations considered for upper and lower limb activities, respectively. The upper and lower limb activities consider all the activity categories which are both limb movements, single limb movement and limb bending. The log-normal PDF parameters μ and σ are presented in each plot for the LOS and NLOS links which depends on the wearable antenna orientation and type of link formed. As observed in Fig. 10 (a) the PDF spread is highest for IN_LOS links for on-body PL measurements and lowest spread is observed for OUT_NLOS links. For σ_τ, highest spread of the data is observed for FR_NLOS links and lowest spread is observed for IN_LOS links which can be predicted from Fig. 10 (b). Considering lower limb movement activities analysis in Fig. 11 (a) for PL measurements, maximum spread of data is observed for IN_LOS and minimum for IN_NLOS. In case of σ_τ, the maximum spread is observed for OUT_NLOS links and minimum for IN_LOS links which can be inferred from Fig. 11 (b).

V. PATH LOSS AND RMS DELAY SPREAD VS. DISTANCE

Variation of PL magnitude with distance is analysed in this section for various orientations (OUT, IN, FR) of the wearable antenna. The distance between various Tx-Rx locations for various postures (based on angle locations) during the physical activities are calculated geometrically by approximating the body model as depicted in Fig. 4 (a)-(b) respectively. The analysis is carried out considering all types of activities for upper and lower limb movements. A least square fit is performed on the measured PL results to obtain the path loss (PL_0) at reference distance and PL exponent denoted by γ. The path loss can be modeled as a function of distance using the following expression [33].

$$PL_{dB}(d) = PL_{dB}(d_0) + 10\gamma \log_{10}\left(\frac{d}{d_0}\right) \quad (5)$$

where, d_0 is the reference distance set to 10 cm for on body channels, path loss (PL_0) is the path loss at reference distance d_0 and γ is the path loss exponent.

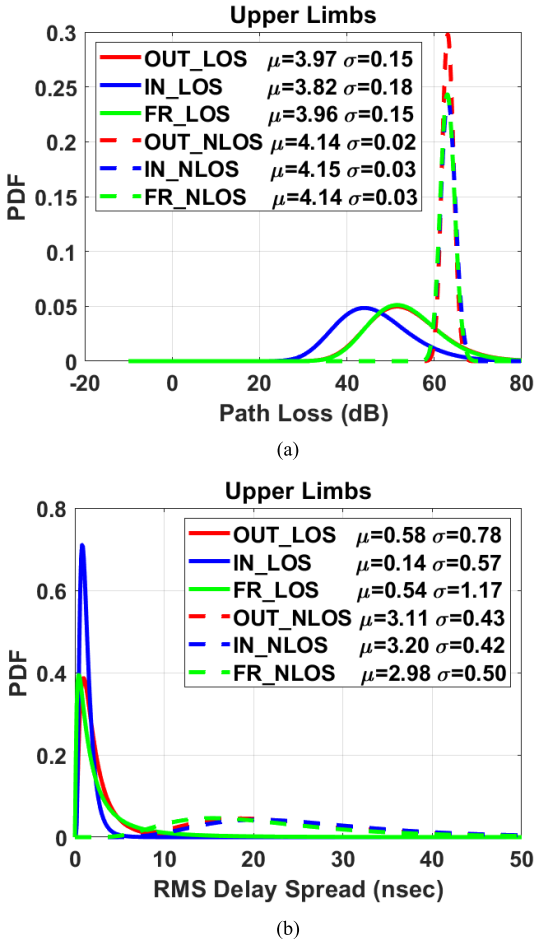

FIGURE 10. Log-normal PDFs of the (a) Path loss and (b) RMS delay spread for various on-body antenna orientations (OUT, IN, FR) during upper limb activities. Solid line represents LOS links and dotted line represents NLOS links.

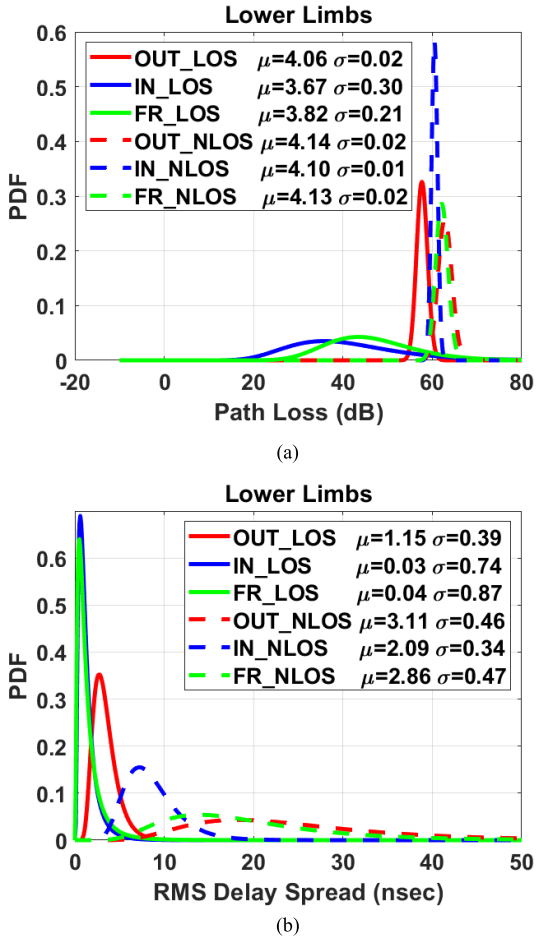

FIGURE 11. Log-normal PDFs of the (a) Path loss and (b) RMS delay spread for various on-body antenna orientations (OUT, IN, FR) during lower limb activities. Solid line represents LOS links and dotted line represents NLOS links.

TABLE 2. Path loss magnitude: arm and leg activity.

	OUT		IN		FR	
	PL_0	γ	PL_0	γ	PL_0	γ
Upper Limbs: (A1-A11)						
LOS	49.55	0.97	36.74	1.95	44.95	1.56
NLOS	59.52	0.45	60.78	0.25	60.53	0.30
Lower Limbs: (L1-L10)						
LOS	45.67	1.58	19.02	3.89	30.20	3.03
NLOS	61.11	0.31	56.56	0.52	56.69	0.66

Path loss magnitude vs distance for LOS and NLOS links is presented in Fig. 12 for FR orientation of the wearable antenna during upper limbs activities. Table 2 summaries the PL_0 and γ values for various orientations and upper/lower limb activities. PL magnitude and PL_0 is higher for NLOS links when compared with LOS links whereas the γ is higher for LOS in comparison to NLOS. This is because the variation in PL magnitude is much larger for LOS links ranging from 25-55 dB in comparison to NLOS links generally ranging between 60-65 dB.

The rms delay spread can also be modeled as a function of Tx-Rx separation distance as the amount of multipath

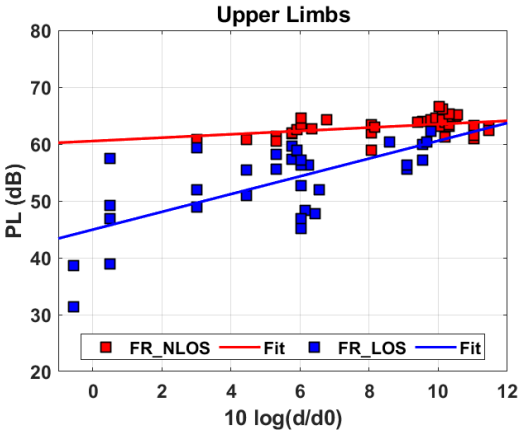

FIGURE 12. Variation of the PL magnitude with distance (measured and modelled) for LOS and NLOS on-body links for FR orientation of the wearable antennas during upper limb activity.

and spread increases with distance. Rms delay spread for various on-body channel links are analyzed for upper and lower limb activities for various orientations of the wearable antennas. Parameters related to the linear fitting model (σ_τ

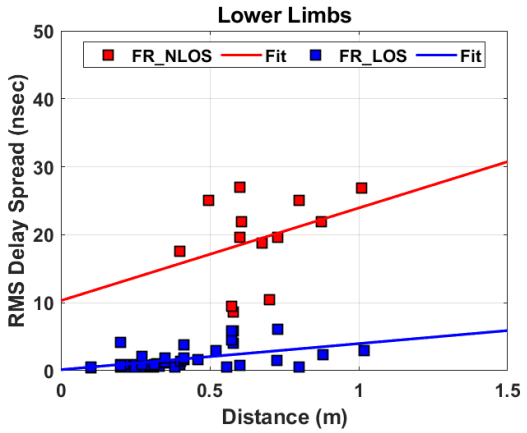

FIGURE 13. Variation of the rms delay spread with distance (measured and modelled) for LOS and NLOS on-body links for FR orientation of the wearable antennas during lower limb activity.

TABLE 3. RMS delay spread: arm and leg activity.

	OUT		IN		FR	
	σ_τ (d=10 cm)	*Slope*	σ_τ (d=10 cm)	*Slope*	σ_τ (d=10 cm)	*Slope*
Upper Limbs: (A1-A11)						
LOS	1.84	2.66	0.52	2.89	1.21	4.37
NLOS	14.89	14.80	22.06	5.09	16.11	8.32
Lower Limbs: (L1-L10)						
LOS	1.16	5.69	0.43	2.39	0.55	3.67
NLOS	20.62	12.06	5.03	5.56	12.77	11.86

($d = 10$ cm) and *Slope*) of the measured values are computed for various on-body links and postures during the limb activities. Comparing LOS and NLOS σ_τ values, the multipath components and spread is much stronger for NLOS links due to the presence of the human subject as obstruction. Fig. 13 depicts the measured and modeled σ_τ values for the LOS and NLOS on-body links for the FR orientation during the lower limb activities. Table 3. summarizes the fitting parameters for various LOS and NLOS for different antenna orientations for upper and lower limb activities. The σ_τ values, σ_τ at $d = 10$ cm and *slope* is higher for NLOS links in comparison LOS links. The on-body NLOS links vary from 10-30 nsec and the LOS links are generally below 6 nsec during various physical activities carried out.

VI. CONCLUSION

In this work on-body channel classification, characterization and modelling has been investigated for various upper and lower limb movements. The on-body channel information can be utilized for tracking and monitoring applications in healthcare domain such as rehabilitation, assisted living, and preventive healthcare. Kurtosis has been found as a very suitable parameter for classification of LOS and NLOS links for upper and lower limbs on-body channel links with an accuracy higher than 98 %. Path loss and rms delay spread on-body statistics, characterization and modelling analysis has been carried out for the various physical exercises. Distance dependent analysis has also been reported showing variation in the results for upper and lower limbs activities. The investigations give insight on various aspects of the variation in on-body channel characteristics for various limb movements, location and orientation of the wearable antennas and suitable placement of the wearable antenna while performing physical exercises.

REFERENCES

[1] S. Seneviratne, Y. Hu, T. Nguyen, G. Lan, S. Khalifa, K. Thilakarathna, M. Hassan, and A. Seneviratne, "A survey of wearable devices and challenges," *IEEE Commun. Surveys Tuts.*, vol. 19, no. 4, pp. 2573–2620, 4th Quart., 2017.

[2] M. Cornacchia, K. Ozcan, Y. Zheng, and S. Velipasalar, "A survey on activity detection and classification using wearable sensors," *IEEE Sensors J.*, vol. 17, no. 2, pp. 386–403, Jan. 2017.

[3] Y. Gu, A. Lo, and I. Niemegeers, "A survey of indoor positioning systems for wireless personal networks," *IEEE Commun. Surveys Tuts.*, vol. 11, no. 1, pp. 13–32, 1st Quart., 2009.

[4] S. Zihajehzadeh and E. J. Park, "A novel biomechanical model-aided IMU/UWB fusion for magnetometer-free lower body motion capture," *IEEE Trans. Syst., Man, Cybern., Syst.*, vol. 47, no. 6, pp. 927–938, Jun. 2017.

[5] R. Bharadwaj and S. K. Koul, "Assessment of limb movement activities using wearable ultra-wideband technology," *IEEE Trans. Antennas Propag.*, vol. 69, no. 4, pp. 2316–2325, Apr. 2021.

[6] T. Kim Geok, K. Zar Aung, M. Sandar Aung, M. Thu Soe, A. Abdaziz, C. Pao Liew, F. Hossain, C. P. Tso, and W. H. Yong, "Review of indoor positioning: Radio wave technology," *Appl. Sci.*, vol. 11, no. 1, p. 279, Dec. 2020.

[7] T. Otim, A. Bahillo, L. E. Díez, P. Lopez-Iturri, and F. Falcone, "Towards sub-meter level UWB indoor localization using body wearable sensors," *IEEE Access*, vol. 8, pp. 178886–178899, 2020.

[8] R. Bharadwaj, S. Swaisaenyakorn, C. G. Parini, J. C. Batchelor, and A. Alomainy, "Impulse radio ultra-wideband communications for localization and tracking of human body and limbs movement for healthcare applications," *IEEE Trans. Antennas Propag.*, vol. 65, no. 12, pp. 7298–7309, Dec. 2017.

[9] J. Hamie, B. Denis, and M. Maman, "On-body localization experiments using real IR-UWB devices," in *Proc. IEEE Int. Conf. Ultra-WideBand (ICUWB)*, Sep. 2014, pp. 362–367.

[10] Y. Qi, C. B. Soh, E. Gunawan, K.-S. Low, and A. Maskooki, "A novel approach to joint flexion/extension angles measurement based on wearable UWB radios," *IEEE J. Biomed. Health Informat.*, vol. 18, no. 1, pp. 300–308, Jan. 2014.

[11] R. Ngah and Y. Zahedi, "UWB communications: Present and future," in *Proc. IEEE Asia–Pacific Conf. Appl. Electromagn. (APACE)*, Dec. 2016, pp. 373–378.

[12] S. K. Meghani, M. Asif, F. Awin, and K. Tepe, "Empirical based ranging error mitigation in IR-UWB: A fuzzy approach," *IEEE Access*, vol. 7, pp. 33686–33697, 2019.

[13] J. F. Schmidt, D. Neuhold, C. Bettstetter, J. Klaue, and D. Schupke, "Wireless connectivity in airplanes: Challenges and the case for UWB," *IEEE Access*, vol. 9, pp. 52913–52925, 2021.

[14] R. Bharadwaj, S. Swaisaenyakorn, C. Parini, J. C. Batchelor, S. K. Koul, and A. Alomainy, "UWB channel characterization for compact L-shape configurations for body-centric positioning applications," *IEEE Antennas Wireless Propag. Lett.*, vol. 19, no. 1, pp. 29–33, Jan. 2020.

[15] S. Yan, P. J. Soh, and G. A. E. Vandenbosch, "Wearable ultrawideband technology—A review of ultrawideband antennas, propagation channels, and applications in wireless body area networks," *IEEE Access*, vol. 6, pp. 42177–42185, 2018.

[16] M. Sarestoniemi, M. Hamalainen, and J. Iinatti, "An overview of the electromagnetic simulation-based channel modeling techniques for wireless body area network applications," *IEEE Access*, vol. 5, pp. 10622–10632, 2017.

[17] K. Turbic, M. Sarestoniemi, M. Hamalainen, and L. M. Correia, "User influence on polarization characteristics in off-body channels," *IEEE Access*, vol. 8, pp. 167570–167584, 2020.

[18] D. B. Smith, D. Miniutti, T. A. Lamahewa, and L. W. Hanlen, "Propagation models for body-area networks: A survey and new outlook," *IEEE Antennas Propag. Mag.*, vol. 55, no. 5, pp. 97–117, Oct. 2013.

[19] A. Alomainy, A. Sani, A. Rahman, J. G. Santas, and Y. Hao, "Transient characteristics of wearable antennas and radio propagation channels for ultrawideband body-centric wireless communications," *IEEE Trans. Antennas Propag.*, vol. 57, no. 4, pp. 875–884, Apr. 2009.
[20] A. Gao, H. Peng, J. Zou, and Z. Cao, "Performance of WBAN UWB system based on the measured on-body channel model," in *Proc. IEEE 2nd Int. Conf. Cloud Comput. Intell. Syst.*, Oct. 2012, pp. 893–897.
[21] S. Sangodoyin and A. F. Molisch, "Experimental characterization of the dependence of UWB personal area networks channels on body mass index," in *Proc. IEEE Int. Conf. Commun. (ICC)*, May 2018, pp. 1–6.
[22] M. SärestÖniemi, C. Kissi, C. P. Raez, M. Sonkki, M. Hämäläinen, and J. Iinatti, "Propagation and UWB channel characteristics on the human abdomen area," in *Proc. 13th Eur. Conf. Antennas Propag. (EuCAP)*, Mar. 2019, pp. 1–5.
[23] S. Sangodoyin and A. F. Molisch, "A measurement-based model of BMI impact on UWB multi-antenna PAN and B2B channels," *IEEE Trans. Commun.*, vol. 66, no. 12, pp. 6494–6510, Dec. 2018.
[24] T. Kumpuniemi, T. Tuovinen, M. Hamalainen, K. Y. Yazdandoost, R. Vuohtoniemi, and J. Iinatti, "Measurement-based on-body path loss modelling for UWB WBAN communications," in *Proc. 7th Int. Symp. Med. Inf. Commun. Technol. (ISMICT)*, Mar. 2013, pp. 233–237.
[25] Q. H. Abbasi, A. Sani, A. Alomainy, and Y. Hao, "Experimental characterization and statistical analysis of the pseudo-dynamic ultrawideband on-body radio channel," *IEEE Antenna Wireless Propag. Lett.*, vol. 10, pp. 748–751, Aug. 2011.
[26] T. Kumpuniemi, M. Hämäläinen, K. Y. Yazdandoost, and J. Iinatti, "Human body shadowing effect on dynamic UWB on-body radio channels," *IEEE Antennas Wireless Propag. Lett.*, vol. 16, pp. 1871–1874, 2017.
[27] B. Sansoda and S. Choomchuay, "An investigation of UWB path loss for body area network," in *Proc. 18th Int. Symp. Commun. Inf. Technol. (ISCIT)*, Sep. 2018, pp. 363–366.
[28] *Range of Motion*. Accessed: Jul. 15, 2021. [Online]. Available: https://www.physio-pedia.com/Range_of_Motion
[29] *Active Range of Motion Exercises*. Accessed: Jul. 15, 2021. [Online]. Available: https://www.drugs.com/cg/active-range-of-motion-exercises.html
[30] S. Marano, W. M. Gifford, H. Wymeersch, and M. Z. Win, "NLOS identification and mitigation for localization based on UWB experimental data," *IEEE J. Sel. Areas Commun.*, vol. 28, no. 7, pp. 1026–1035, Sep. 2010.
[31] A. Fort, C. Desset, P. De Doncker, P. Wambacq, and L. Van Biesen, "An ultra-wideband body area propagation channel model-from statistics to implementation," *IEEE Trans. Microw. Theory Techn.*, vol. 54, no. 4, pp. 1820–1826, Jun. 2006.
[32] T. S. Rappaport, *Wireless Communications Principles and Practice*. Upper Saddle River, NJ, USA: Prentice-Hall, 1996.
[33] A. F. Molisch, K. Balakrishnan, C. C. Chong, S. Emami, A. Fort, J. Karedal, J. Kunisch, H. Schantz, U. Schuster, and K. Siwiak, *IEEE 802.15.4a Channel Model-Final Report*, Standard 802.15-04-0662-01-04a, IEEEP802.15 Working Group for Wireless Personal Area Network (WPANs), Sep. 2004.

RICHA BHARADWAJ (Member, IEEE) received the B.E. degree (Hons.) in electronics and communication from Panjab University, Chandigarh, India, in 2008, the M.S. degree in micro and nanotechnologies for integrated systems from the Politecnico di Torino, Turin, Italy, INPG Grenoble, Grenoble, France, and EPFL Lausanne, Lausanne, Switzerland, in 2010, and the Ph.D. degree in electronic engineering with the specialization in ultra-wideband technology from the Antennas and Electromagnetics Research Group, School of Electronics and Computer Science, Queen Mary University of London, London, U.K., in 2015. She was a National-Postdoctoral Fellow (Science and Engineering Research Board, Department of Science and Technology, Government of India) with the Centre for Applied Research in Electronics, Indian Institute of Technology Delhi, New Delhi, India, from 2016 to 2018, where she has been working as a Postdoctoral Fellow. She has authored or coauthored two book chapters and a number of research publications in leading international journals and peer-reviewed conferences. Her current research interests include ultra-wideband communication, 3-D localization, wireless sensor networks, body centric communication, radio propagation characterization and modeling, miniaturized antenna design, and flexible and wearable communication.

She serves as a reviewer for several leading transactions and journals in the field of antennas and propagation, wireless communication, sensors, and vehicular technology. She was awarded the C. J. Reddy Best Paper Award for Young Professionals from the Indian Conference on Antennas and Propagation (INCAP 2019), Ahmedabad, India.

SHIBAN K. KOUL (Life Fellow, IEEE) received the B.E. degree in electrical engineering from Regional Engineering College, Srinagar, India, in 1977, and the M.Tech. and Ph.D. degrees in microwave engineering from Indian Institute of Technology Delhi, New Delhi, India, in 1979 and 1983, respectively. He has been an Emeritus Professor with Indian Institute of Technology Delhi, since 2019, and the Mentor Deputy Director (strategy and planning, international affairs) with IIT Jammu, Jammu and Kashmir, India, since 2018. He served as the Deputy Director (strategy and planning) with IIT Delhi, from 2012 to 2016. He also served as the Chairman for Astra Microwave Products Limited, Hyderabad, from 2009 to 2019, and the Dr. R. P. Shenoy Astra Microwave Chair Professor with IIT Delhi, from 2014 to 2019. His research interests include RF MEMS, high-frequency wireless communication, microwave engineering, microwave passive and active circuits, device modeling, millimeter and sub-millimeter wave IC design, body area networks, flexible and wearable electronics, medical applications of sub-terahertz waves, and reconfigurable microwave circuits, including miniaturized antennas. He has successfully completed 38 major sponsored projects, 52 consultancy projects, and 61 technology development projects. He has authored/coauthored 521 research papers, 15 state-of-the art books, four book chapters, and two e-books. He holds 23 patents, six copyrights, and one trademark. He has guided 26 Ph.D. theses and more than 120 master's theses.

Prof. Koul is a fellow of INAE and IETE. He is currently the Chief Editor of *IETE Journal of Research* and an Associate Editor of the *International Journal of Microwave and Wireless Technologies* (Cambridge University Press). He served as a Distinguished Microwave Lecturer for IEEE MTT-S for the period 2012–2014. Prior to this, he served as a Speaker Bureau Lecturer for IEEE MTT-S. He also served as an AdCom Member for the IEEE MTT-S, from 2010 to 2018, and is presently a member of the Awards, Nomination and Appointments, MGA, M&S, and Education committees of IEEE MTT-S. He was a recipient of numerous awards, including the IEEE MTT Society Distinguished Educator Award (2014), the Teaching Excellence Award (2012) from IIT Delhi, the Indian National Science Academy (INSA) Young Scientist Award (1986), the Top Invention Award (1991) of the National Research Development Council for his contributions to the indigenous development of ferrite phase shifter technology, the VASVIK Award (1994) for the development of Ka-band components and phase shifters, the Ram Lal Wadhwa Gold Medal (1995) from the Institution of Electronics and Communication Engineers (IETE), the Academic Excellence Award (1998) from Indian Government for his pioneering contributions to phase control modules for Rajendra Radar, the Shri Om Prakash Bhasin Award (2009) in the field of electronics and information technology, the VASVIK Award (2012) for the contributions made to the area of information, communication technology (ICT), and the M. N. Saha Memorial Award (2013) from IETE.